Free Energy Profiles for Na^+ Adsorption on a Metal Electrode

Tooru Matsui[†] and William L. Jorgensen*

Contribution from the Department of Chemistry, Yale University, New Haven, Connecticut 06511.
Received September 23, 1991

Abstract: Monte Carlo statistical mechanics simulations have been used to determine free energy profiles for the approach of a sodium ion to a model metal electrode in aqueous solution and in tetrahydrofuran (THF). The ion and 200-300 solvent molecules are explicitly represented in a periodic cell bounded in the $\pm z$ directions by soft walls that are polarizable via image charges. Statistical perturbation theory provided the free energy profiles from the wall out 8-10 Å into the solvent. In both cases, a single minimum is found corresponding to the sodium ion with its first shell of solvent molecules in contact with the wall. At least for the case of an uncharged electrode, the traditional model of a layer of adsorbed water between the solvated ion and the electrode appears incorrect. The structure of the interfacial solvent and the changes in solvation of the ion as it approaches the wall are also considered in detail.

Introduction

The arrangement of solvent molecules and ions near the surface of an electrode is a fundamental issue in electrochemistry. The current view for aqueous systems is well described by Bockris and Reddy;[1] a layer of oriented water molecules is adsorbed along with some larger, typically negatively charged ions, while smaller cations with their first solvent shell intact are separated from the electrode by the primary water layer. The centers of the adsorbed and second-layer ions are said to form the inner and outer Helmholtz planes. No direct experimental structural data are available to support the model; however, the model is consistent with electrochemical measurements and rough estimates of the cost in free energy for specific adsorption of ions from the outer Helmholtz layer.[2] On the theoretical side, the most sophisticated calculations to date for the distribution of ions near a model electrode were carried out by Torrie et al.[3] They used a large hard sphere with variable charge to represent the electrode and solved for the ion distribution via the RHNC integral equation theory. The shapes of the solvent molecules are considered in these calculations in an average sense, though they are not explicitly represented. Consequently, no atomically detailed structural results on the disposition of water molecules were obtained. In order to represent a metal electrode it is also important to allow it to be fully polarizable. This is typically achieved through image charges,[4] which were not implemented in the RHNC studies. The problem has been readdressed in the present work using Monte Carlo statistical mechanics with explicit representation of the solvent molecules in the presence of a classical metallic wall including image charges. Potentials of mean force have been obtained for approach of the sodium ion to the wall in both aqueous solution and tetrahydrofuran (THF), a medium of interest for long-life batteries. These results and details on the orientation of water near the wall and the ion provide new insights on the structure of the double layer.

Computational Details

Monte Carlo Simulations. The calculations were carried out on systems containing a single sodium ion plus 324 water molecules or 192 THF molecules in a rectangular box with dimensions 18.7 × 18.7 × 31.0 Å for water and 25.8 × 25.8 × 43.1 Å for THF. Smooth, Lennard-Jones walls were placed at the $\pm z$ boundaries, and periodic boundary conditions were implemented in the x and y directions. The z dimensions were chosen to give the experimental density for the bulk solvent with allowance for the thickness of the walls. The canonical (NVT) ensemble was employed at 25 °C along with Metropolis and preferential sampling.[5] The latter caused the solvent molecules nearest the ion to be moved 2-3 times as often as the most distant solvent molecules.

The changes in free energy were computed from statistical perturbation theory (eq 1)[6] as the sodium ion was moved in increments of 0.1 Å from the left wall in the $+z$ direction. In the expression, the perturbation is made from position i to j where E_j and E_i are the total potential

$$A_j - A_i = -k_B T \ln \langle \exp[-(E_j - E_i)/k_B T] \rangle_i \quad (1)$$

energies and the average is obtained from sampling configurations for position i. Double-wide sampling was applied, so two free energy changes were computed in each simulation corresponding to the ion at $(0,0,z)$ being perturbed to $(0,0,z - 0.1$ Å) and $(0,0,z + 0.1$ Å). With the two-body potential functions used here, the total energy difference consists of the change in the ion-solvent (E_{SX}), solvent-wall (E_{SB}), and ion-wall (E_{XB}) energies, while there is no change in the solvent-solvent (E_{SS}) energy for the perturbation.

The initial configurations for the solvent were taken from equilibrated boxes of the bulk solvent, and the ion was inserted. Runs for new ion positions were then started from the last configuration for the previous position. For water, at each position, the system was equilibrated for (2-4) × 10^6 configurations and the averaging covered an additional 8 × 10^6 configurations. For THF, (1-2) × 10^6 configurations of equilibration were followed by 5 × 10^6 configurations of averaging. These long simulations were undertaken to provide high precision for the free energy changes and in response to the observations of Valleau and Gardner on convergence difficulties in Monte Carlo simulations of pure water between hard and metallic walls.[4] In runs of the present length and system size for pure water between metallic walls, we obtained good symmetry in the O and H atom distributions about the center of the cell. The difficulties in the earlier work may be related to the smaller system size of 125 molecules and, as the authors noted, to the use of the minimum image method rather than the spherical truncation of interactions as performed here.

New configurations were generated by randomly selecting a solvent molecule, randomly translating it in all three Cartesian directions, and randomly rotating it about one randomly chosen Cartesian axis. The ranges for the motions were selected to give an overall acceptance rate of 40-50% for new configurations.

Potential Functions. The ion-solvent and solvent-solvent interactions were described in the Coulomb plus Lennard-Jones format of eq 2 where i and j are sites on the ion or molecule (a and b), q is the charge, and r_{ij} is the intersite distance. The combining rules for the Lennard-Jones

$$\Delta E_{ab} = \sum_i \sum_j (q_i q_j e^2/r_{ij} + A_{ij}/r_{ij}^{12} - C_{ij}/r_{ij}^6) \quad (2)$$

parameters are $A_{ij} = (A_{ii}A_{jj})^{1/2}$ and $C_{ij} = (C_{ii}C_{jj})^{1/2}$ where A_{ii} and C_{ii} can be described in terms of Lennard-Jones σ's and ϵ's as $A_{ii} = 4\epsilon_i\sigma_i^{12}$ and $C_{ii} = 4\epsilon_i\sigma_i^6$. Previously reported parameters were used for the sodium ion[7a] and for the solvent molecules, namely, the TIP4P and OPLS models for water and THF.[8,9] TIP4P has four sites with the center of negative

[†] Permanent address: Matsushita Electric Industrial Co., Energy Research Laboratories, Moriguchi, Osaka 570, Japan.

(1) Bockris, J. O'M.; Reddy, A. K. N. *Modern Electrochemistry*; Plenum Press: New York, 1970; Vol. 2.
(2) Bockris, J. O'M.; Devanathan, M. A. V.; Muller, K. *Proc. R. Soc. London, A* **1963**, *274*, 68. Bode, D. D., Jr. *J. Phys. Chem.* **1972**, *76*, 2915.
(3) Torrie, G. M.; Kusalik, P. G.; Patey, G. N. *J. Chem. Phys.* **1988**, *89*, 3285. Torrie, G. M.; Kusalik, P. G.; Patey, G. N. *J. Chem. Phys.* **1989**, *90*, 4513. Torrie, G. M.; Kusalik, P. G.; Patey, G. N. *J. Chem. Phys.* **1989**, *91*, 6367.
(4) Valleau, J. P.; Gardner, A. A. *J. Chem. Phys.* **1987**, *86*, 4162. Gardner, A. A.; Valleau, J. P. *J. Chem. Phys.* **1987**, *86*, 4171.
(5) (a) Metropolis, N.; Rosenbluth, A. W.; Rosenbluth, M. N.; Teller, A. H.; Teller, E. *J. Chem. Phys.* **1953**, *21*, 1087. (b) Owicki, J. C. *ACS Symp. Ser.* **1978**, No. 86, 159.
(6) Zwanzig, R. W. *J. Chem. Phys.* **1954**, *22*, 1420.
(7) (a) Chandrasekhar, J.; Spellmeyer, D. C.; Jorgensen, W. L. *J. Am. Chem. Soc.* **1984**, *106*, 903. (b) Chandrasekhar, J.; Jorgensen, W. L. *J. Chem. Phys.* **1982**, *77*, 5080.
(8) Jorgensen, W. L.; Chandrasekhar, J.; Madura, J. D.; Impey, R. W.; Klein, M. L. *J. Chem. Phys.* **1983**, *79*, 926.

0002-7863/92/1514-3220$03.00/0

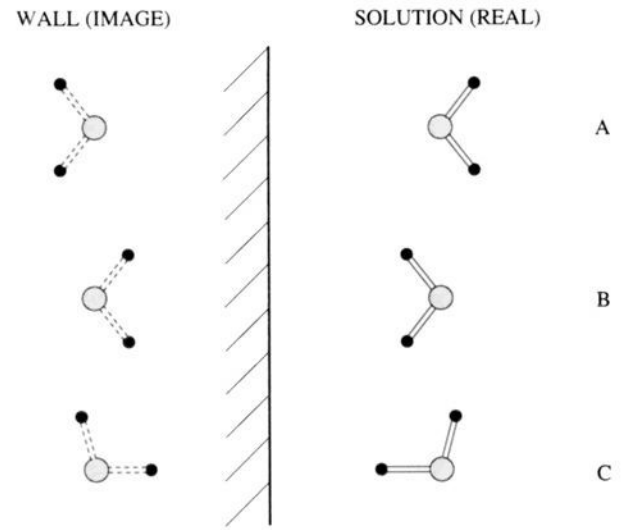

Figure 1. Sample orientations for a water molecule and its image near a metallic wall.

charge displaced from the oxygen by 0.15 Å, and the OPLS model for THF has five sites centered on the nuclei with the hydrogens implicit. The internal geometries of the solvent molecules were not altered during the simulations and the THF molecules were planar, as in the earlier studies that generated the parameters to yield properties of the pure liquids in accord with experiment.[8,9]

The ion–wall and solvent–wall interactions consisted of Lennard-Jones (eq 3) and image (eq 4) terms. In this case, the Lennard-Jones part is

$$\Delta E_{LJ} = (2\pi/3)\rho\sum_i \sigma_{iw}^3\epsilon_{iw}[(2/15)(\sigma_{iw}/z_i)^9 - (\sigma_{iw}/z_i)^3] \quad (3)$$

$$\Delta E_{image} = (1/2)\sum_i\sum_j q_i q_j e^2/r_{ij} \quad (4)$$

integrated over the wall, ρ is the number of wall atoms per unit volume, and z_i is the perpendicular distance from the centers of the surface layer of wall atoms to the ion or solvent sites. Previously reported parameters for the wall were adopted corresponding to graphite with $\rho = 0.114$ Å^{-3}, $\sigma_w = 3.4$ Å, and $\epsilon_w = 0.055$ kcal/mol.[10] The Lennard-Jones parameters in eq 3 were then obtained for the different pairs as $\sigma_{iw} = (\sigma_i\sigma_w)^{1/2}$ and $\epsilon_{iw} = (\epsilon_i\epsilon_w)^{1/2}$.

Classical metallic walls with an infinite dielectric constant were included at both ends of the box through the image charge potential.[4] The walls are polarized by the solution; this induces a field that is equivalent to that obtained by having image charges of opposite sign and equal magnitude located at a distance behind the surface that is equal to the distance between the surface and the real sites in front of it. Thus, for each site in the solution, its usual interactions with the other sites in the solution are evaluated along with its image interaction with its own image and with the images of all other sites behind the wall. In eq 4, the index i is for the real sites and j is for the image sites, r_{ij} is the distance between them, and the factor of 2 is associated with the fact that there is no electric field within the metal. A final addition was to add hard spheres with a radius of 1.25 Å to the hydrogens of water for their interaction with the walls; this is necessary to avoid unreasonably close approach of the hydrogens to the walls since in the TIP4P model only the oxygen of water is a Lennard-Jones site. The hydrogen radius was chosen to be consistent with the Lennard-Jones σ for hydrogen in all-atom models of hydrocarbons.[11]

With these potential functions, the optimal interaction of an isolated sodium ion occurs 1.7 Å from the wall with an energy of −47.0 kcal/mol. For wall–water interactions, three sample orientations including their images are illustrated in Figure 1. The corresponding energy curves versus the wall–O distances are very similar, as shown in Figure 2; there is no preference for orientations with hydrogens pointed toward or away from the wall. The minima occur at 2.7 Å with well depths of ca. −1.3 kcal/mol. In the implementation of Gardner and Valleau,[4] the optimal attraction of water to the wall is much stronger at −5.7 kcal/mol and

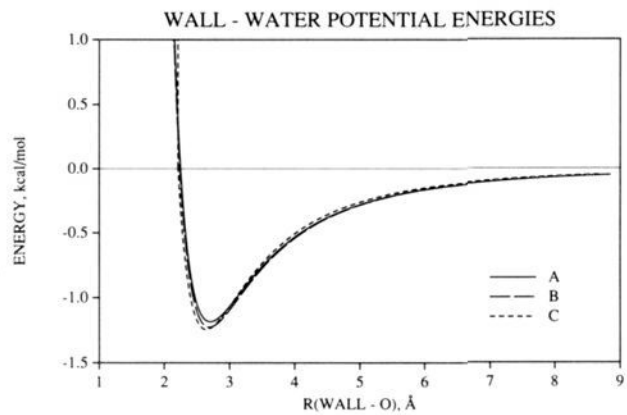

Figure 2. Computed interaction energies for a water molecule oriented as in Figure 1 with the metallic wall. Distances are in angstroms and energies in kilocalories/mole throughout.

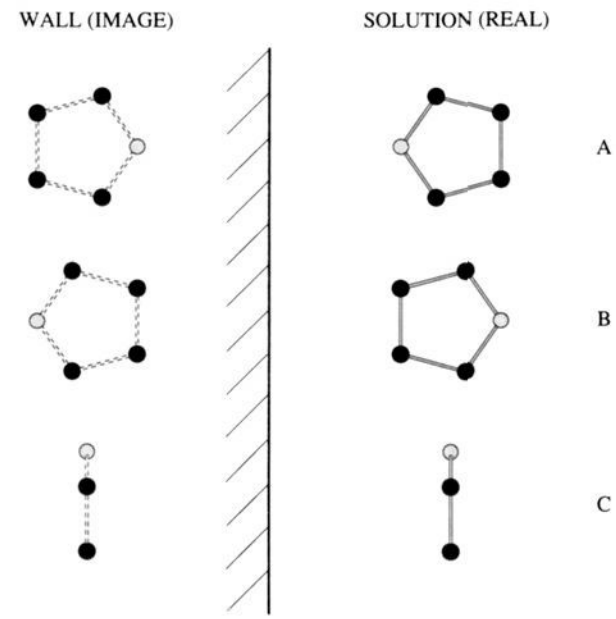

Figure 3. Sample orientations for a THF molecule and its image near a metallic wall.

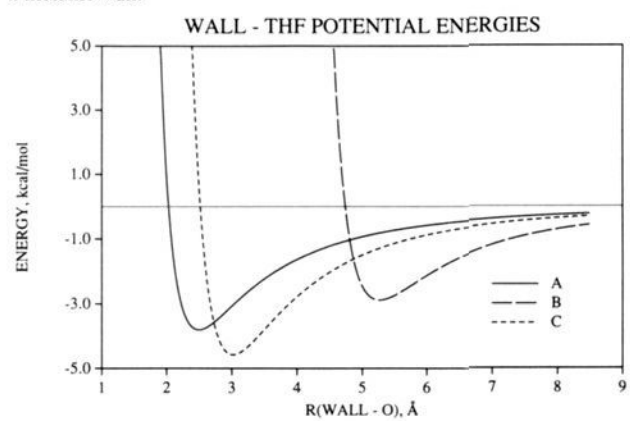

Figure 4. Computed interaction energies for a THF molecule oriented as in Figure 3 with the metallic wall.

overly favors orientation of hydrogens toward the wall.[12] This follows from their placement of a hard sphere only on the fourth site near oxygen of the TIPS2 model with no repulsive terms centered on the hydrogens. Three orientations for THF near the wall are shown in Figure 3, with

(9) Briggs, J. M.; Matsui, T.; Jorgensen, W. L. *J. Comput. Chem.* **1990**, *11*, 958.
(10) Crowell, A. D.; Steele, R. B. *J. Chem. Phys.* **1961**, *34*, 1347.
(11) Jorgensen, W. L.; Severance, D. L. *J. Am. Chem. Soc.* **1990**, *112*, 4768. Jorgensen, W. L.; Briggs, J. M. *J. Am. Chem. Soc.* **1989**, *111*, 4190.
(12) Raghavan, K.; Foster, K.; Motakabbir, K.; Berkowitz, M. *J. Chem. Phys.* **1991**, *94*, 2110. Spohr, E. *J. Phys. Chem.* **1989**, *93*, 6171.

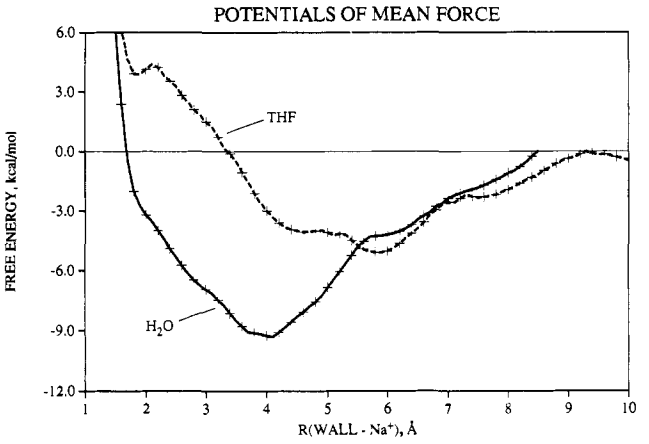

Figure 5. Computed free energy profiles (potentials of mean force) for the approach of sodium ion to the metallic wall in aqueous solution and in THF. The curves have been zeroed at 8.5 Å in water and 10.0 Å in THF.

the corresponding energy curves in Figure 4. The closest approach of oxygen to the wall is achieved in orientation A, while the global minimum occurs for a slightly tilted version of the parallel form C with a well depth of −4.7 kcal/mol at a wall–O distance of 2.9 Å.

In the Monte Carlo simulations, the interactions in the aqueous and THF solutions were spherically truncated at cutoff distances of 9.0 and 12.0 Å with quadratic feathering to 0 over the last 0.5 Å. The cutoffs for the solvent–solvent and solvent–ion interactions were based on the O–O and O–ion distances, for both the real and image interactions. Substantial testing with even longer cutoffs for selected wall–ion separations did not yield significant effects on the computed free energies. Corrections for the long-range electrostatic interactions neglected beyond the cutoffs were not included for this reason and because Gardner and Valleau had found that their dipole sheets procedure yielded a correction of less than 0.1% of the total energy for water between hard walls.[4] The present calculations were carried out on Silicon Graphics 4D/35 workstations with a version of the BOSS program modified to include the polarizable walls.[13]

Results and Discussion

Potentials of Mean Force. The key results are shown in Figure 5, which gives the change in free energy as a function of the distance of the sodium ion from the wall. The calculations were carried out to 8.5 Å in water and 10.0 Å in THF; the potentials of mean force (pmfs) were zeroed at these points, though asymptotic behavior has not been achieved, particularly for the aqueous system. The uncertainty in the zeroing for the aqueous case could be several kilocalories/mole. Before further discussion of the results, the convergence characteristics in Figure 6 should be noted. The three curves show the pmf after averaging for 1×10^6, 5×10^6, and 8×10^6 configurations for each increment in the ion's position for the more difficult aqueous system. The qualitative behavior is established at 1×10^6 configurations, and the similar results at 5×10^6 and 8×10^6 configurations give confidence in the quantitative convergence.

Both pmfs show one principal minimum. For water, the minimum occurs at a wall–ion distance of 4.1 Å with a well depth of −9 kcal/mol, keeping in mind the uncertainty in the zeroing. This is much farther than the optimal distance of 1.7 Å found in the absence of solvent, so the ion is not making direct contact with the wall, consistent with the traditional view of small cations staying outside the inner Helmholtz plane.[1,2] The well is surprisingly deep and indicates a very strong preference for sodium ion to populate the region 3–5 Å from the wall. The RHNC results also yielded a strong preference of ca. 2 kcal/mol for sodium to be about 0.7 solvent diameter from an uncharged large sphere.[3] Much of the difference can be attributed to the ion–wall image attraction in the present case. The well depth is still surprising and may be affected by several issues. First, the classical image charge approach may overstate the polarization effects at

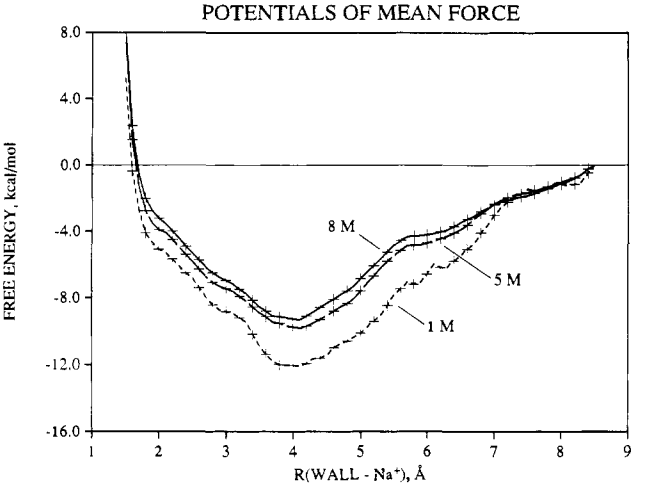

Figure 6. Computed free energy profiles for the approach of sodium ion to the metallic wall in aqueous solution after 1×10^6, 5×10^6, and 8×10^6 configurations of averaging for each increment in the ion's position. All curves have been zeroed at 8.5 Å.

the atomic level. Second, the present calculations correspond to infinite dilution; the presence of additional ions at finite concentrations should provide some screening. Furthermore, limitations in the present potential functions including the use of fixed charges and the incomplete zeroing are other sources of potential error. Nevertheless, these calculations still represent the most sophisticated treatment of such systems to date, and the qualitative results, which are consistent with the RHNC findings, seem reasonable in view of the structural results discussed below.

The minimum is pushed out to 5.9 Å in THF, broadened and made shallower with a maximum depth of −5.1 kcal/mol. Again, the favored position for the sodium ion is not in contact with the wall. As fully revealed below, the minima correspond to having the first solvent shell intact and touching the wall. The reason the minimum is out farther in THF then simply reflects the larger size of a THF than a water molecule. The greater well depth for water is also related to the size difference. Figure 7 shows the four energy components, solvent–solvent, solvent–ion, solvent–wall, and ion–wall, for the aqueous and THF systems as a function of ion–wall distance. The components with the walls include the image contributions. Each curve has been zeroed at its farthest extent, so the relative energies are given for easier comparison. The statistics are excellent for all curves, as reflected in their smoothness, except for the solvent–solvent term in water, which is noisier. Approach of the ion to the wall is favored by the solvent–solvent term (solvent is released from the ion) and by the ion–wall interaction to similar extents. The solvent–wall term is almost constant, but becomes slightly less favorable when the ion is close to the wall, presumably owing to restrictions placed on the water positions by the ion. And, naturally, the ion–solvent energy becomes less favorable as the ion has to shed solvent molecules near the wall. Interestingly, the solvent–wall and ion–wall energy curves are nearly the same in water and THF. The solvent–solvent terms also have the same trend and, in fact, do not directly enter the free energy expression (eq 1). The principal difference between THF and water is in the ion–solvent energy curves. Because THF is larger, the first solvent shell of THF cannot remain intact as close to the wall as for water. The earlier loss of first-shell solvent causes the ion–solvent energy to rise earlier for THF and results in the shallower minimum at larger distance to the wall.

In closing this section, it may be noted that the prior work most closely related to this one technically was a Monte Carlo effort that yielded the pmf for a Lennard-Jones particle approaching a Lennard-Jones wall in water.[14] Two minima were found corresponding to the Lennard-Jones particle being in contact with

(13) Jorgensen, W. L. BOSS, Version 2.9. Yale University, New Haven, CT, 1990.

(14) Wallqvist, A.; Berne, B. J. *Chem. Phys. Lett.* **1988**, *145*, 26.

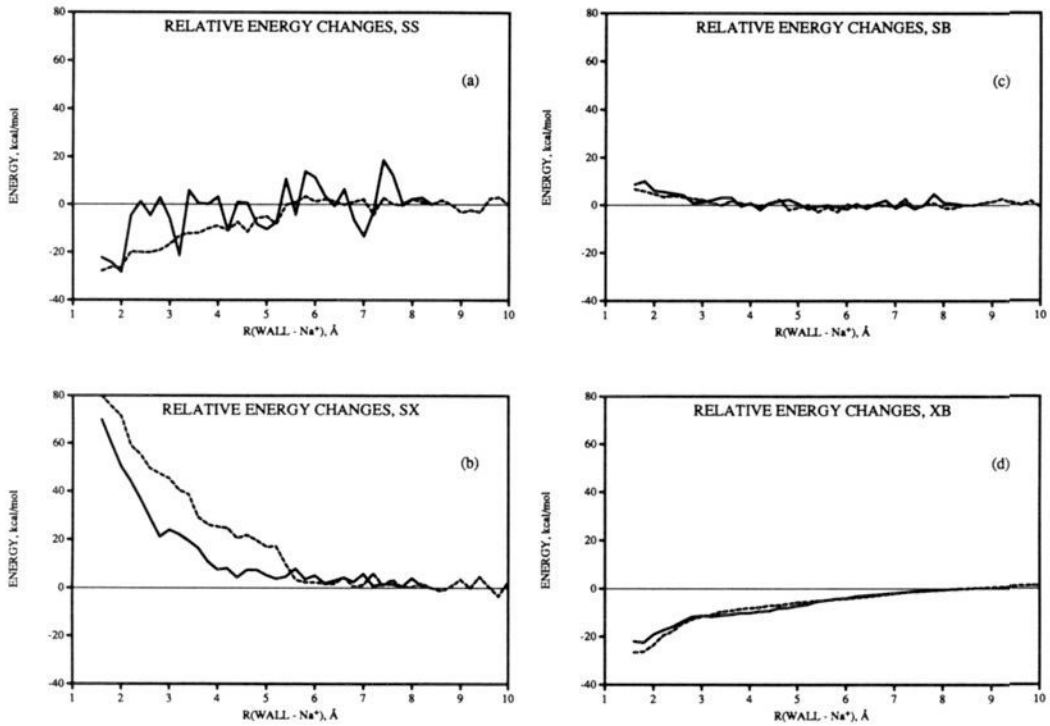

Figure 7. Computed potential energy components as a function of the sodium ion's distance to the metallic wall in water (solid lines) and in THF (dashed lines). (a) The solvent–solvent energy. (b) The solvent–ion energy. (c) The solvent–wall energy. (d) The ion–wall energy. The results are given relative to the values at 8.5 Å in water and 10.0 Å in THF.

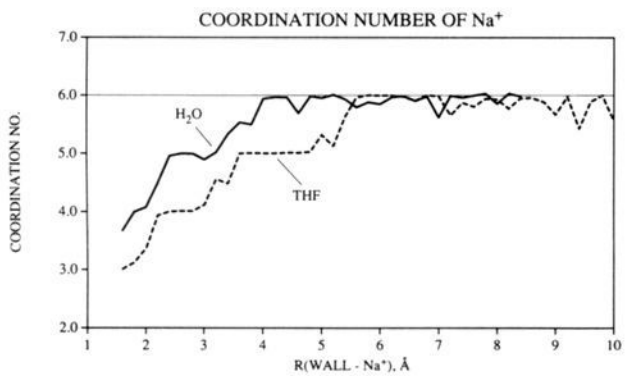

Figure 8. Variation in numbers of first-shell solvent molecules for the sodium ion as a function of distance to the metallic wall in water (solid curve) and THF (dashed curve).

the wall or separated from it by one water molecule.

Ion Solvation. The ion–oxygen radial distribution functions far from the wall show a sharp first peak that integrates to six solvent molecules for both water and THF. Six-coordination was found in earlier computations for sodium ion in the bulk solvents[7] and has also been obtained from diffraction experiments for Na^+ in water.[15] The changes in coordination numbers as the ion approaches the wall are revealed in Figure 8. For THF, six-coordination is maintained up to the minimum in the pmf; five-coordination then ensues about 5 Å from the wall, and the pmf turns up. The next clear break in the pmf occurs around 4 Å, where four-coordination sets in and the free energy rises steeply. Similarly, for water, the loss of six-coordination, now shifted in to 4 Å, coincides with the upturn in the pmf at the minimum. A change in slope for the pmf is also apparent near 2 Å, where the coordination number drops to 4. Thus, there is close correspondence between the changes in primary solvation of the ion and the free energy profiles.

(15) Neilson, G. W.; Enderby, J. E. *Annu. Rep. Prog. Chem., Sect. C* **1979**, *76*, 185.

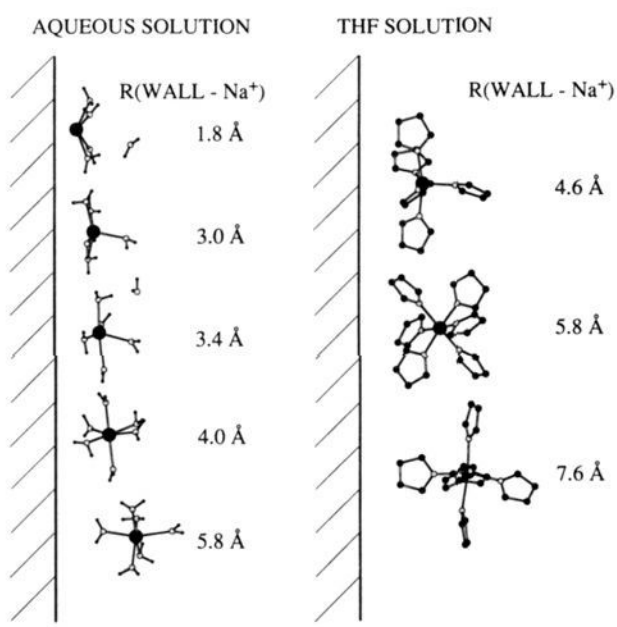

Figure 9. Illustration of the change in first-shell solvation for the sodium ion as it approaches the metallic wall in water (left) and in THF (right).

Detailed distributions for the wall–ion–oxygen angles were computed for the first-shell molecules as a function of distance to the wall. Figure 9 shows the ion and neighboring solvent molecules in arrangements selected from the simulations that are consistent with the angular distributions. In water at 5.8 Å, the ion is octahedrally coordinated and an apical water is directed at the wall. For the minimum at 4.0 Å, an equatorial edge of the octahedron now faces the wall; there is insufficient space for a water molecule to be fully inserted between the wall and ion. At 3.4 and 3.0 Å, a water molecule has been shed and the ion directly faces the wall. Finally, when forced to 1.8 Å, only four water molecules remain coordinated to the ion and they are bent back away from the wall. The progression is similar in THF. At

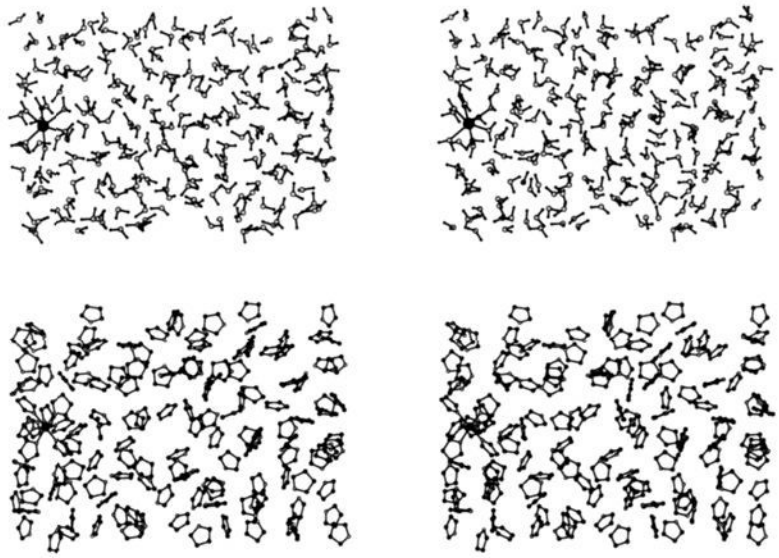

Figure 10. Stereoplots of arbitrary configurations from the Monte Carlo simulations for sodium ion in the aqueous (top) and THF (bottom) solutions. The metallic walls are at both horizontal boundaries; periodic boundary conditions apply in the two orthogonal directions. The sodium ion is 4.0 Å from the left wall in the aqueous system and 5.8 Å from the left wall in the THF system, i.e., near the minima in the potentials of mean force (Figure 5).

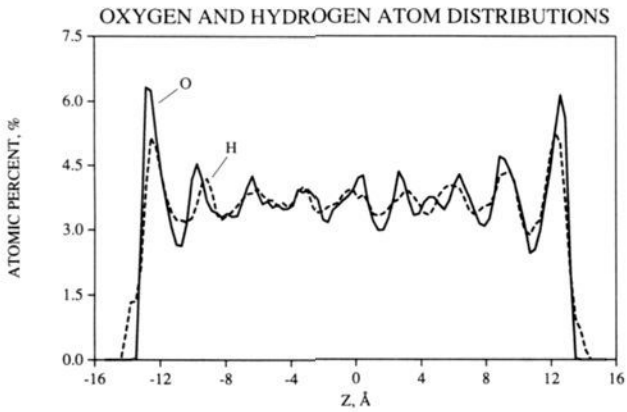

Figure 11. Distribution of O and H atom densities for water across the simulation cell. The metallic walls are at ±15.5 Å, and the sodium ion is 4.0 Å from the left wall at −11.5 Å.

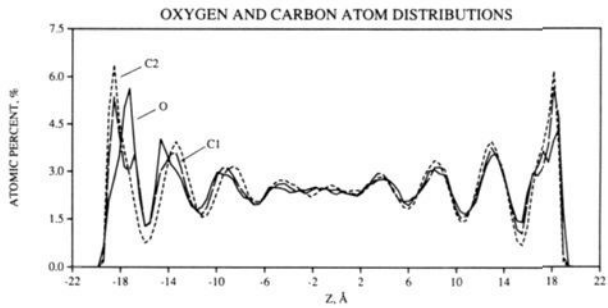

Figure 12. Distributions of O, C1, and C2 atom densities for THF across the simulation cell. The metallic walls are at ±21.55 Å, and the sodium ion is 5.8 Å from the left wall at −15.75 Å.

7.6 Å an apical THF separates the ion from the wall. The octahedron then rotates to place a triangular face toward the wall near the minimum in the pmf, and the coordination number drops to 5 at 4.6 Å with loss of an apical THF.

These descriptions are also consistent with stereoplots of the simulation cells. An example is shown for both systems in Figure 10 with the sodium ion near the minima in the pmfs. Solvent molecules more than 5 Å for water and 8 Å for THF in front of the ion have been removed from the stereoplots for ease of viewing the ion. The octahedral coordination is apparent with an edge or face directed toward the wall. Importantly, these results are not consistent with the traditional view that a layer of water molecules separates the electrode surface from the first shell of solvent molecules around a small cation to create the outer Helmholtz plane. The view presented here is that the first shell of solvent molecules around the cation directly contacts the electrode surface. Naturally, these findings can be affected by the presence of other ions and charging of the electrode; however, the present results correspond to the important limit of no charge and high dilution.

Solvent Structure. The calculated atomic density distributions for the solvent molecules across the simulation cells are shown for water and THF in Figures 11 and 12 when the ion is near the minima in the pmfs. These distributions were computed using every configuration in the simulations ("on the fly"). Even with the ion present, the symmetry about the middle of the cells is quite good. This reflects the fact that the number of solvent molecules closely associated with the ion is relatively small in systems with the present size. In both cases, there are approximately nine layers of solvent between the walls. There is a buildup of solvent density adjacent to the walls which gradually dampens out, though it only fully dampens out in the longer THF cell nearly 20 Å from the walls. The buildup near the walls has been observed in previous simulations of water between walls,[4,12,14,16,17] though the extent is somewhat greater here owing to the image interactions. For water, the peak positions in the O and H distributions largely coincide, though a small fraction of hydrogens manage to get a little closer to the walls than the oxygens. For THF, at the right wall, there is no preference for the occurrence of one solvent atom type over any other; however, the presence of the sodium at z = −15.8 Å causes the first and second oxygen peaks near the left wall to tilt in toward the ion.

The hydrogen bonding for water molecules in the aqueous system was also analyzed from configurations saved roughly every 50 000 steps during the simulations. Our findings in this area and for angular distributions are similar to those of Lee et al. for ST2 water between Lennard-Jones walls.[17] We define a hydrogen bond by a water–water interaction energy of −2.25 kcal/mol or less.[8] The simulation cell was then divided into 10 slices, each 3.1 Å

(16) (a) Jonsson, B. *Chem. Phys. Lett.* **1981**, *82*, 520. (b) Marchesi, M. *Chem. Phys. Lett.* **1983**, *97*, 224. (c) Zhu, S.-B.; Robinson, G. W. *J. Chem. Phys.* **1991**, *94*, 1403.

(17) Lee, C. Y.; McCammon, J. A.; Rossky, P. J. *J. Chem. Phys.* **1984**, *80*, 4448.

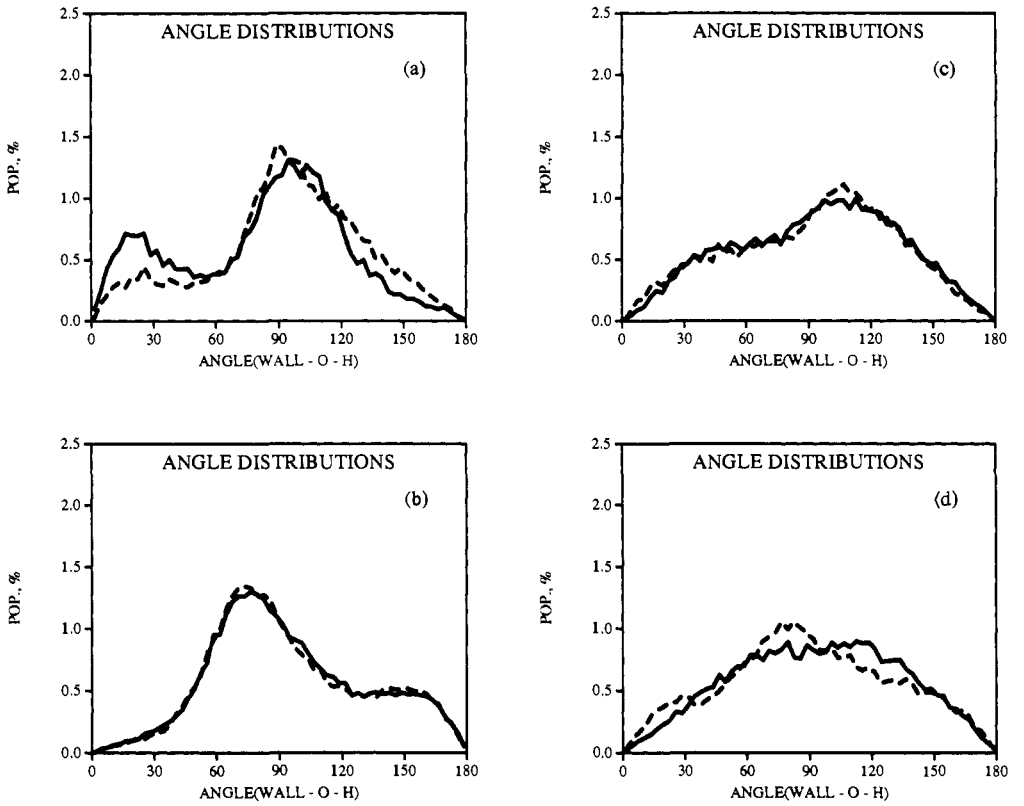

Figure 13. Distributions for the wall–O–H angle in the aqueous system. The sodium ion is 4.0 Å from the left metallic wall. The results for four solvent slices are shown, as described in the text, progressing out from the walls. The solid and dashed curves are for the corresponding slices near the left and right walls, respectively.

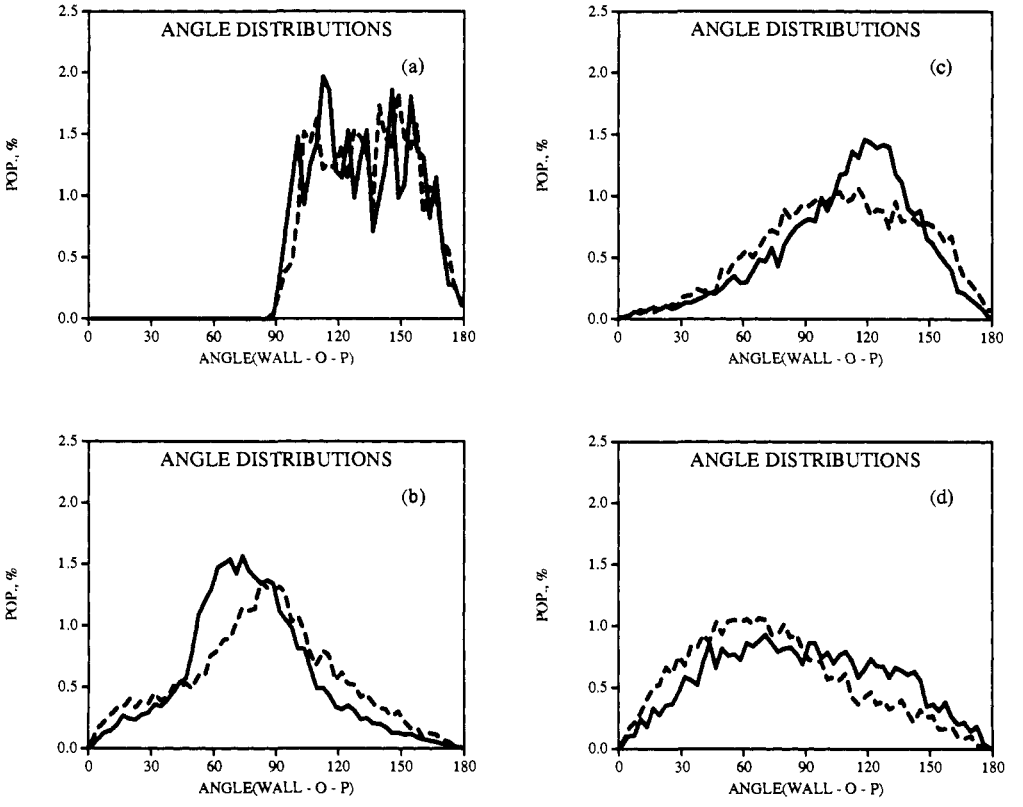

Figure 14. Distributions for the wall–O–P angle in the THF system where P is the midpoint of C1 and C4. The sodium ion is 5.8 Å from the left metallic wall. The results for four solvent slices are shown, as described in the text, progressing out from the left (solid curves) and right (dashed curves) walls.

thick, perpendicular to the z axis. Except for the two slices adjacent to the walls, the hydrogen-bond numbers, energetics, and angular characteristics are indistinguishable from those of bulk water independent of the position of the ion. The average number of hydrogen bonds is 3.6, the average strength is −4.1 kcal/mol, and the average O–H···O angle (θ) is 157°. In fact, the hydrogen

bonds for the water molecules within 3.1 Å of the walls also have the same average strength and θ; however, the average number of hydrogen bonds is reduced by 0.8 to 2.8.

The distributions of wall···O–H angles were also computed from the saved configurations. The results when the ion is 4.0 Å from the left wall are shown for four slices in Figure 13. The first slice is from the wall to the position of the first peak in the oxygen distribution (z = −15.5 to −12.7 Å), the second is from the first peak to the first valley (z = −12.7 to −10.8 Å), the third is from there to the second peak position (z = −10.8 to −9.4 Å), and the fourth is from the second peak to the second valley (z = −9.4 to −8.2 Å). The solid and dashed curves in the figure are for the slices extending from the left ($-z$) and right ($+z$) walls. The distributions are essentially the same for either wall, so the effects of the ion near the left wall are highly localized. In view of the solid angle element, the curves in Figure 13 would all show sine dependence if there were no orientational preferences for the wall···O–H angles. Such behavior is being approached for the fourth slice (Figure 13d). However, in the first slice (Figure 13a), there is a significantly enhanced probability of finding a hydrogen pointed toward the wall as reflected in the low-angle band near 20°. There is also enhancement reflected in the peak near 100°, which is consistent with pointing a lone-pair position toward the wall. The curves for the second slice are roughly the mirror image of those for the first slice; now the enhancement is for pointing a hydrogen away from the wall. This same pattern was obtained by Lee et al., and their analysis remains appropriate.[17] They interpreted the water structure near the wall as reminiscent of ice I with the c axis normal to the surface. Their paper should be consulted for details. A lone pair or hydrogen points toward the wall, which results in the loss of one hydrogen bond for the water molecules closest to the wall. The ice I structure makes the first peak in the oxygen density distribution actually consist of a "doubled" layer of water separated by ca. 0.9 Å. The outer half of this layer for an ideal tetrahedral system would have three hydrogen-bonding groups pointed at 71° to the wall and one at 180°, while the inner part of the layer closest to the wall would have three groups at 109° and one at 0°. These tendencies are consistent with the patterns in parts b and a, respectively, of Figure 13, though the model is clearly idealized. There is much disorder in the present fluid systems as compared to an ice crystal, which is obvious in Figure 10.

For the THF system, the wall–dipole angular distributions can be considered. They were constructed from the saved configurations using the wall–O–P angle where P is the midpoint between C1 and C4. The results for four slices analogous to the aqueous case (wall to first peak in the O density distribution, first peak to first valley, first valley to second peak, and second peak to second valley) are shown in Figure 14 for the case where the sodium ion is 5.8 Å from the left wall at z = −15.8 Å. The solid and dashed curves are again for the slices working out from the left and right walls, respectively. The results from the two sides are similar. The ion is between the second and third slices, which can account for the differences between the dashed and solid curves in parts b and c of Figure 14. In order to point toward the ion, THF molecules in the second slice would have oxygen atoms pointed away from the wall and those in the third slice would point toward the wall. This translates into a preference for smaller wall–O–P angles in the second slice and larger ones in the third slice from the left wall (solid curves). Overall, beyond the first slice, the intrinsic sine dependence for the distributions becomes apparent. Interestingly, the THF closest to the wall avoids having oxygen atoms directed into the wall. This is reasonable since the dipolar ends of the molecules are then kept oriented outward so they can interact most favorably with other THF molecules. However, in view of the image forces, it was not obvious a priori that this would be the case.

Conclusion

The realistic simulation of an ion near an electrode in solution has been advanced in the present work by the explicit inclusion of solvent molecules, the use of image potentials, and the calculation of potentials of mean force by the latest methods. Great detail was obtained on the changes in free energy and in solvation of sodium ion as it approaches the model electrode. A strong preference was found in both water and THF solution for sodium ion to reside with its first solvation shell in contact with the electrode's surface. Thus, the outer Helmholtz plane is predicted to reside about 1 solvent diameter closer to the electrode than has been commonly accepted. On the technical side, though lengthy simulations are required, convergence for atom density profiles and for potentials of mean force in such interfacial systems was found not to be fundamentally problematic. The calculations can be refined and extended through consideration of other ions and through enhancements of the potential functions and electrode model. The present results stand as a reference for future simulation work and will hopefully encourage additional efforts in clarifying the disposition of ions and solvent molecules near electrodes.

Acknowledgment. Gratitude is expressed to the National Science Foundation and Matsushita Electric Industrial Company for support of this work. Discussions with Prof. Michael J. Weaver were also most helpful.

Registry No. THF, 109-99-9; $Na(H_2O)_6^+$, 40791-39-7; $Na(C_4H_8O)_6^+$, 73587-41-4; sodium, 7440-23-5.